Plasmin Desensitization of the PAR1 Thrombin Receptor: Kinetics, Sites of Truncation, and Implications for Thrombolytic Therapy†

Athan Kuliopulos,*,‡ Lidija Covic,‡ Stacy K. Seeley,‡ Paul J. Sheridan,‡ Jari Helin,§,|| and Catherine E. Costello§

Molecular Cardiology Research Institute, Division of Hematology/Oncology, New England Medical Center and Departments of Medicine and Biochemistry, Tufts University School of Medicine, Boston, Massachusetts 02111, and Mass Spectrometry Resource, Boston University School of Medicine, Boston, Massachusetts 02118

Received October 16, 1998; Revised Manuscript Received January 20, 1999

ABSTRACT: It has been hypothesized that protease-activated receptors may be activated and attenuated by more than one protease. Here, we explore a desensitization mechanism of the PAR1 thrombin receptor by anticoagulant proteases and provide an explanation to the enigma of why plasmin/tissue plasminogen activator (t-PA) can both activate and deactivate platelets prior to thrombin treatment. By using a soluble N-terminal exodomain (TR78) as a model for the full-length receptor, we were able to unambiguously compare cleavage rates and specificities among the serum proteases. Thrombin cleaves TR78 at the $R_{41}-S_{42}$ peptide bond with a k_{cat} of 120 s^{-1} and a K_M of 16 μM to produce TR62 (residues 42−103). We found that, of the anticoagulant proteases, only plasmin can rapidly truncate the soluble exodomain at the R70/K76/K82 sites located on a linker region that tethers the ligand to the body of the receptor. Plasmin cleavage of the TR78 exodomain is nearly equivalent to that of thrombin cleavage at R41 with similar rates ($k_{cat} = 30$ s^{-1}) and affinity ($K_M = 18$ μM). Specificity was demonstrated since there is no observed cleavage at the five other potential plasmin-cleavage sites. Plasmin also cleaves the TR78 exodomain at the R41 thrombin-cleavage site generating transiently activated exodomain. We directly demonstrated that plasmin cleaves these same sites in full-length membrane-embedded receptor expressed in yeast and COS7 fibroblasts. The rate of plasmin truncation is similar between the extensively glycosylated COS7-expressed receptor and the nonglycosylated yeast-produced receptor. Mutation of the R70/K76/K82 sites to A70/A76/A82 eliminates plasmin truncation and desensitization of thrombin-dependent Ca^{2+} signaling and converts PAR1 into a plasmin-activated receptor with full agonist activity for plasmin. Plasmin does not desensitize the Ca^{2+} response of platelets or COS7 cells to SFLLRN consistent with intermolecular ligand-binding sites being located to the C-terminal side of K82. Truncation of the wild-type receptor at the C-terminal plasmin-cleavage sites removes the N-terminal tethered ligand or preligand, thereby providing an effective pathway for PAR1 desensitization in vivo.

The PAR1 thrombin receptor (TR or PAR1)[1] is the first identified member of a growing class of protease-activated seven transmembrane receptors which includes PAR2 (*36*), PAR3 (*14*), and PAR4 (*19*, *51*). Thrombin cleaves PAR1 at the $R_{41}-S_{42}$ peptide bond (*47*) located within the long exodomain. The new N-terminal amino acid residues, S_{42}-$FLLRN_{47}$, function as an intramolecular ligand that activates the receptor by a poorly understood conformational change involving the exodomain and possibly extracellular loops (*1*, *9*, *34*). Once cleaved by thrombin, the intramolecular tethered ligand−receptor complex will transduce the signal to a G-protein until the receptor is either cleared from the membrane surface and/or deactivated by some other process. Activation and desensitization of the receptor must be well-controlled because of the potential physiologic damage that would result from unchecked signaling due to thrombin-cleaved receptor. Since cleavage of the receptor at the $R_{41}-S_{42}$ peptide bond is an irreversible proteolytic event, a major question to be addressed is how is this "permanently activated" receptor turned-off?

One pathway to desensitization of signals arising from PAR1 is receptor-mediated endocytosis following phosphorylation of Ser/Thr residues located in the C-terminal cytoplasmic domain of the receptor (*16*, *49*). In endothelial cells, up to 40% of the receptors either remain on the surface or are recycled, but these receptors do not respond to thrombin, nor do they self-activate. Thrombin-cleaved plate-

† This work was supported by NIH R29 GM52926-01, the PEW Scholars Program in the Biomedical Sciences, and the American Society of Hematology (A.K.); NIH P41 RR10888, Thermo BioAnalysis Ltd. (C.E.C.), and the Academy of Finland (J.H.).

* To whom correspondence should be addressed at the Division of Hematology/Oncology and Molecular Cardiology Research Institute, Box 832, New England Medical Center. Fax: (617) 636-4833. E-mail: akuliopu@opal.tufts.edu.

‡ Tufts University School of Medicine.

§ Boston University School of Medicine.

|| Present Address: Protein Chemistry Laboratory, Institute of Biotechnology, University of Helsinki, Finland.

[1] Abbreviations: TR, PAR1 thrombin receptor; PAR, protease-activated receptor; TR78, PAR1 residues 26−103; TR62, PAR1 residues 42−103; FRE, fibrinogen recognition exosite of thrombin; AAA-R70A/K76A/K82A, PAR1 mutant; MALDI-TOF, matrix-assisted laser desorption/ionization time-of-flight; TRAP, thrombin receptor activating peptide.

10.1021/bi9824792 CCC: $18.00
Published on Web 03/19/1999

let receptors are not internalized and remain on the surface in a desensitized state (*35*), suggesting that mechanisms other than phosphorylation and endocytosis may regulate PAR1. One explanation for the class of non-self-activating receptors is that the N-terminal ligand has been altered or hidden within a protected environment (*12*, *35*).

An alternative pathway to receptor desensitization may be proteolytic truncation at the C-terminal side of the ligand or preligand. A major clue to understanding how PAR1 might be desensitized by a proteolytic mechanism is to consider the ability of thrombin to self-regulate its procoagulant activities—namely by activating protein C and the fibrinolytic system. Under normal circumstances, fibrin deposition causes conversion of plasminogen to plasmin by the plasminogen activators t-PA and u-PA. Once formed, plasmin commences degradation of the fibrin polymer for acute purposes of clot dissolution. The ability of plasmin to dissolve blot clots has prompted the development of t-PA derivatives as the therapeutic agent of choice for patients with myocardial infarction or massive pulmonary embolism. Although these thrombolytic agents have led to a considerable decrease in the mortality rate, significant limitations remain including an incidence of cerebral hemorrhage in 1−2% of patients and acute coronary reocclusion in 10% of patients (*4*, *41*). These untoward complications have been ascribed to impaired platelet function (*10*, *41*). The high concentrations of plasmin-generating systems (e.g., the ternary complex of plasminogen, t-PA, and fibrin) on the surface of activated cells make plasmin a prime candidate (*33*, *45*) to mediate desensitization of PAR1. However, the effects of plasmin on platelet function are seemingly contradictory. Plasmin generation has been shown to both activate and inhibit platelets depending on the concentration and duration of plasmin treatment (*27*, *38*). Many studies of the effect of plasmin on cytosolic free calcium in rat C6 glioma cells (*45*), human endothelial cells (3), and human platelets (*20*, *33*) reveal that (a) plasmin, by itself, causes a modest and gradual increase in cytosolic Ca^{2+}; and (b) pretreatment with plasmin attenuates the thrombin response by inhibiting thrombin binding directly.

Other proteases including cathepsin G (*21*, *31*), aminopeptidase M (*5*), tryptase (*30*), granzyme A (*43*), and elastase (*12*, *21*) have also been hypothesized to be involved in attenuation of the thrombin response in platelets (*33*) and endothelial cells (*3*, *39*). The large number of potential targets and accessory binding proteins on the surfaces of these cells, including PAR1−4, makes it more difficult to interpret whole cell proteolysis experiments. We chose to study the kinetics of activation and deactivation of PAR1 by serum proteases using three systems. The first system employed a soluble TR78 exodomain that contains all thrombin-interacting sites including the high-affinity fibrinogen recognition exosite-binding region (*17*), the receptor preligand (*47*), and possibly a portion of the ligand-binding site (*1*, *9*). The second system utilized full-length, nonglycosylated PAR1 expressed on yeast membranes. The third system used full-length, glycosylated receptor expressed on the surface of COS7 fibroblasts. Our laboratory has tested the anticoagulant proteases and now has the first direct evidence for efficient plasmin recognition and cleavage at an exodomain linker region that completely clips off the tethered ligand and would explain some of these unresolved issues.

EXPERIMENTAL PROCEDURES

Materials. Human α-thrombin (3433 NIH units/mg), human Lys-plasmin (2.8 units/mg, >95% pure by SDS−PAGE; 1 unit will hydrolyze 1 μmol of Spectrozyme PL/min), human activated protein-C (8.8 units/mg, >98% pure by SDS−PAGE; 1 unit will hydrolyze 1 μmol of Spectrozyme TH/min), and rabbit lung thrombomodulin (1.02 mol of thrombomodulin/mol of thrombin, K_d = 1.12 nM) were from Hematologic Technologies (Essex Junction, VT). Human α_2-antiplasmin (5 IU/mg, 95% pure by SDS−PAGE) was from American Diagnostica (Greenwich, CT). Human tissue plasminogen activator (50 IU/mg, >95% pure by SDS−PAGE) was from Calbiochem. Restriction enzymes and Vent DNA polymerase were from New England Biolabs (Beverly, MA). Fluorescein isothiocyanate (FITC)-conjugated goat antibodies to rabbit and mouse IgG were purchased from Dako A/S (Glostrup, Denmark). Restriction enzymes were purchased from New England Biolabs (Beverly, MA). Diethylaminoethyl (DEAE) dextran, dimethyl sulfoxide (DMSO), and chloroquine were purchased from Sigma.

Production of Soluble PAR1 Exodomains. Human PAR1 exodomain, TR78 (residues 26−103), was produced in *Escherichia coli* as the C-terminal portion of a fusion protein attached to a 125 amino acid residue bacterial carrier protein, ketosteroid isomerase (KSI), by established procedures (*26*). The polymerase chain reaction was used to amplify PAR1 DNA encoding residues A_{26}−L_{103} using human PAR1 cDNA as template (kindly provided by Shaun Coughlin). *Nco*I and *Xho*I restriction sites were placed at 5′ and 3′ ends of the coding sequence, respectively. A L103M mutation was incorporated within the 3′ primer during the PCR reaction to place a methionine just upstream of the C-terminal His_6 tag. The *Nco*I-*Xho*I PCR fragment was ligated to the *Nco*I/*Xho*I sites of pET22-KFMH (*26*) to create pET22-KTRMH. Sanger dideoxynucleotide sequencing confirmed mutations and ruled out adventitious errors incurred by PCR. The KSI-TR78-M-His_6 fusion construct was produced in *E. coli* strain BL21(DE3)pLysS and purified from inclusion bodies under denaturing conditions by nickel-chelate chromatography. Free TR78 exodomain was released from carrier KSI and His_6 tag by CNBr cleavage at flanking methionines. Preparative reverse-phase HPLC of crude CNBr-cleavage reactions was performed on a 22 × 250 mm 10 μm Vydac C18 column. Pure receptor exodomain was collected, lyophilized, and stored as a fluffy white powder at −80 °C and was stable for at least 1 year. Crude TR78 was quantitatively cleaved with thrombin at R41 to produce TR62. Typical large-scale cleavage reactions consisting of 250 μM TR78, 10 nM thrombin, in 150 mM NaCl, 20 mM KPO_4, pH 7.5 (PBS), were incubated at room temperature for 1 h and quenched with base. TR62 was purified by preparative HPLC and stored as a lyophilized powder at −80 °C. TR78 and TR62 exodomains were sequenced by Edman degradation and were shown to have the correct N-terminal sequence from residues A_{26}−N_{49}, and S_{42}−K_{51}, respectively. The molecular weights were verified by mass spectrometry.

Kinetics of Serum Protease Cleavage of the PAR1 Exodomain. The kinetics of serum protease cleavage of receptor exodomains, TR78 and TR62, were confirmed by HPLC analysis of cleavage peptide products. The assignments of

these peptides were established by mass spectrometry. Lyophilized TR78 or TR62 exodomain was reconstituted in PBS and the concentration determined by UV absorption using an extinction coefficient, $\epsilon_{278} = 15\,200\ M^{-1}\ cm^{-1}$, calculated for a polypeptide containing 2 Trp and 3 Tyr residues. Serum proteases were diluted with prechilled PBS/0.1% PEG-6000 just prior to use and kept on ice. Cleavage reactions were carried out in PBS at 37 °C and initiated by the addition of protease. Initial velocities were obtained by reverse-phase HPLC analysis at 278 nm of base-quenched aliquots removed at early time points where <10% of the starting material was cleaved. Quantitation of cleavage peptide products and starting materials at each time point were determined by the integration of peptide peaks. Since the aromatic amino acid (Trp and Tyr) spectral contributions are additive under the acidic conditions of 0.1% trifluoroacetic acid (*23*), the concentrations of all peptide peaks (except TR16) were calculated using extinction coefficients of each peptide fragment at 278 nm. The concentration of TR16, which lacked Trp and Tyr residues, was measured at 222 nm by comparison with equimolar TR62 generated by quantitative thrombin cleavage (10 nM) of 50 μM TR78 for 10 min. The TR62 concentration was independently determined by absorption at 278 nm.

Kinetic constants, k_{cat}, and K_M, of cleavage at the P1−P5 plasmin-cleavage sites of TR78 and TR62 were determined from data taken over 4 h periods. The kinetics of the disappearance of starting material and the kinetics of cleavage at the P1, P2 + P3, P1 + P2 + P3, and P5 plasmin-cleavage sites at early times were determined directly by the method of initial rates (*8*). Determination of kinetic constants, k_{cat} and K_M, at each secondary thrombin-cleavage site of TR62 was obtained by kinetic simulation for data taken over 4 h periods. Simulations were performed by numerical integration with the program KINSIM v3.3 (*2*) on a Silicon Graphics Indigo^2 workstation (Mountain View, CA). A 2-site kinetic model of thrombin (T) secondary cleavage is as follows:

$$\begin{aligned}
&TR62 + T \overset{K_1}{\longleftrightarrow} T_1TR62 \overset{k_2}{\longrightarrow} T + TR57 + TR5;\\
&TR62 + T \overset{K_3}{\longleftrightarrow} T_2TR62 \overset{k_4}{\longrightarrow} T + TR27 + TR35;\\
&T + TR57 \overset{K_5}{\longleftrightarrow} T_2TR57 \overset{k_6}{\longrightarrow} T + TR30 + TR27;\\
&T + TR35 \overset{K_7}{\longleftrightarrow} T_1TR35 \overset{k_8}{\longrightarrow} T + TR30 + TR5;\\
&T + TR27 \overset{K_9}{\longleftrightarrow} T_2TR27;\ T + TR30 \overset{K_{10}}{\longleftrightarrow} T_1TR30 \quad (1)
\end{aligned}$$

The bound thrombin species T_1 and T_2 represent active site binding at R46- and K76-cleavage sites, respectively. The last two equilibrium reactions, governed by constants K_9 and K_{10}, represent the contribution of thrombin binding to the final cleavage peptide products in the overall reaction. These two product inhibition reactions were necessary additions to the model in order to fit the data taken at longer time points where the TR30 and TR27 products predominate.

Mass Spectrometry. Matrix-assisted laser desorption/ionization (MALDI) mass spectra were recorded on a Finnigan MAT Vision 2000 reflectron time-of-flight (TOF) mass spectrometer (Thermo BioAnalysis, Hemel Hempsted, UK), using a Laser Science Inc. (Newton, MA) nitrogen laser (337 nm, 5 ns pulse width). The samples were dissolved in water (1−5 pmol/μL), and 1 μL of this solution was mixed with 1 μL of the matrix solution (10 g/L 2,5-dihydroxybenzoic acid in water) on a stainless steel probe tip. The drop was dried with a gentle stream of air before the probe was inserted into the ion source. A 5 kV accelerating voltage and a 5 kV postacceleration voltage at the detector were used. Spectra were recorded at 500 MHz as single shots; several spectra were added together to achieve good signal-to-noise ratios. Under the experimental conditions used, peptides appear as protonated molecular ions $[M + H]^+$. For abundant species, the doubly protonated molecular ion $[M + 2H]^{2+}$ is also observed. In most cases, external calibration with protein standards was used; in some cases, internal standards were used. Mass assignment accuracy is within 0.1% with external standards and 0.01% with internal standards.

Production of PAR1 in Yeast. The construction of the yeast expression plasmid containing His_6T7-tagged PAR1, p112-H6T7TR (TRP1 2 μm), is described elsewhere (*42*). The triple alanine mutant (R70K76K82 → A70A76A82) was assembled from 5′ and 3′ DNA fragments as follows. By using PCR, we amplified the 5′ fragment from the human PAR1 cDNA in pBluescript with primers (+) 5′-CGCTCTAGAGGATCCTTAGATCCCCGGTCATTTCTT-3′ and (−) 5′-GGAATTCACTCGAGGCATTGATGGAGACTAATGCGTATTCAGTT-3′. The 3′ PCR fragment was amplified with primers (+) 5′-CCGGATCCGCCTCGAGTCCTCTTCAAGCACAACTTCCTGC-3′ and (−) 5′-GGCGGTACCTCAATGCATCTCAGAGGAAGCGTAATAGTAAAT-5′. The 5′ PCR product was digested with *Bam*HI and *Xho*I, and the 3′ PCR product was digested with *Xho*I-*Pst*I. The two fragments were ligated into the *Bam*HI-*Pst*I sites of p112-H6T7TRΔ379 (*42*) to create p112-AAA-TRΔ379. The *Pst*I-*Eco*RI fragment from p112-H6T7TR was inserted into the identical sites of p112-AAA-TRΔ379 to create the p112-AAA-TR yeast expression plasmid. A detailed description of the preparation and proteolytic treatment of yeast membranes containing PAR1 is given in a separate report (*42*).

Production of PAR1 in COS7 Fibroblasts. We made two different PAR1 constructs for the COS7 cell transfection experiments: full-length wild-type (WT) and triple alanine mutant R70K76K82 → A70A76A82 (AAA) tagged with a N-terminal His_6T7 epitope with a consensus Kozak sequence placed at the 5′ end of the gene for efficient mammalian translation (*22*). Both PAR1 constructs have been inserted into the mammalian expression vector pDEF3 which places PAR1 under the control of a human EF-1α promoter and carries a Neomycin selectable marker (*11*). PCR was used to amplify the human PAR1 cDNA in pBluescript with primer (+) 5′-TTTGGATCCGCAGAGCCCGGGACAATGG-3′ and (−) 5′-TTTTCTAGACTAAGTTAACAGCTTTTTG-TATAT-3′. The AAA mutant was constructed in the same manner except p112-AAA-TR served as template.

Cytosolic Calcium Measurements. COS7 cells were detached from flasks with 1.5 mM EDTA in PBS for 5−15 min. Cells were resuspended and washed in KRB buffer (118 mM NaCl, 1 mM $CaCl_2$, 1 mM KH_2PO_4, 1.2 mM $MgSO_4 \cdot 7H_2O$, 1 mg/mL BSA, 0.72 mg/mL dextrose, 20 mM Hepes, pH 7.2). Cells were loaded with 2.5 μM fura-2/AM (Molecular Probes) for 30 min at 37 °C, 5% CO_2, with gentle shaking for platelets and vigorous shaking for COS7 cells. After thorough washing in KRB buffer, cells were resuspended in fresh KRB buffer at ~1 × 10^6 cells/mL.

Table 1: Identification of PAR1 Exodomain Protease-Cleavage Peptides by MALDI−Time-of-Flight Mass Spectrometry

substrate	protease[a]	cleavage product	residues	predicted mass (*m*/*z*)	observed mass (*m*/*z*)
TR78	thrombin	TR16	26−41	1783	1783
		TR27	77−103	2929	2929
		TR30	47−76	3646	3644
		TR35	42−76	4263	4262
		TR57	47−103	6556	6553
		TR62	42−103	7174	7170
TR62	plasmin	TR21	83−103	2288	2288
		TR27	77−103	2929	2929
		TR29	42−70	3608	3606
		TR33	71−103	3584	3584
		TR35	42−76	4263	4261
		TR41	42−82	4903	4901
TR78	plasmin	TR21	83−103	2288	2288
		TR27	77−103	2929	2928
		TR29	42−70	3608	3606
		TR33	71−103	3584	3584
		TR35	42−76	4263	4263
		TR38	33−70	4548	4547
		TR44	33−76	5203	5204
		TR45	26−70	5373	5372
		TR51	26−76	6028	6027
		TR62	42−103	7174	7178
		TR71	33−103	8114	8115
TR78	activated protein C	TR62	42−103	7174	7166

[a] Protease concentrations were as follows: 1 μM thrombin, 10 nM plasmin, and 200 nM activated protein C. Cleavage reactions were conducted as described in the Figure 1 legend.

Fluorescence was measured in a Perkin-Elmer LS50B spectrofluorimeter. The florescence emission was recorded at 510 nm and dual excitation at 340 and 380 nm. Platelet Ca^{2+} experiments were performed without stirring at 25 °C; COS7 cells were stirred at 300 rpm with a magnetic microstir bar. At the end of each experiment, the Ca^{2+} concentration was calibrated by the addition of 12 mM EGTA followed by 0.38 mM digitonin plus 15 mM $CaCl_2$.

Antibodies and Flow Cytometry. The polyclonal antibody (SFLLR-Ab) directed against the thrombin receptor ligand region, residues 42−55, was generated by previously described methods (*24*). Briefly, the peptide S_{42}FLLRNP-NDKYEPF$_{55}$C was synthesized, purified by HPLC, conjugated to maleimide-activated keyhole limpet hemocyanin (Pierce), and antisera-produced from two rabbits (Rockland, Gilbertsville, PA). Polyclonal antibodies were purified from rabbit antisera using a SFLLRNPNDKYEPFC peptide-Sepharose 4B affinity column. The T7 tag mouse monoclonal antibody (T7-Ab) directed against residues MASMTG-GQQM was purchased from Novagen. For flow cytometry experiments, COS7 cells transfected with WT-PAR1 or AAA-PAR1 were grown for 48 h. The cells were washed twice with serum-free DMEM, and twice with phosphate-buffered saline (PBS) and incubated with various concentrations of Lys-plasmin, or thrombin for 15 min at 37 °C, 5% CO_2. After being washed with cold FACS buffer (1% FCS in PBS, 0.2% azide), cells were centrifuged at 200*g* at 4 °C for 5 min. Pelleted cells were resuspended in 200 μL of FACS buffer and incubated with SFLLR-Ab (1:400) or T7-Ab (1:100) for 30 min at 4 °C. Cells were washed three times with FACS buffer, resuspended in 200 μL of FACS buffer, and incubated with secondary antibody for 30 min at 4 °C using either goat antirabbit IgG-FITC(6 μg/mL; Zymed) or goat antimouse IgG-FITC antibodies (10 μg/mL; DAKO). Cells were then washed three times in FACS buffer and fixed with 1% formaldehyde solution in FACS buffer. Cells were analyzed for fluorescence with a FACScan flow cytometer (Becton Dickinson).

RESULTS

Production of Soluble PAR1 Exodomains. To produce soluble PAR1 exodomains, we eliminated the N-terminal signal peptide (PAR1 residues 1−25) and terminated the exodomain at residue 103 just prior to the first transmembrane helix. Replacement of residues 1−35 with a prolactin signal peptide has no effect on receptor function when expressed in *Xenopus* and mammalian cells (*18*). TR78 (residues 26−103) was produced in 100 mg quantities as a fusion protein in *E. coli* sandwiched between a small carrier protein and a polyhistidine (His_6) tag. Following nickel-chelate chromatography, TR78 was released from both carrier protein and His_6 tag by chemical cleavage with CNBr at junctional methionine residues and purified to homogeneity by HPLC. Edman sequencing and MALDI-TOF mass spectrometry (Table 1) confirmed that the amino acid sequence of TR78 was correct. The activated TR62 exodomain was produced by quantitative cleavage by thrombin at R41 and likewise shown to have the correct amino acid sequence (Table 1). Lyophilized TR78 and TR62 exodomains were refolded in PBS buffer and were shown to have defined structure by circular dichroism and NMR spectroscopy.[2]

Functional Characterization of Soluble PAR1 Exodomains. We first wanted to establish that the soluble TR78 exodomain is an authentic thrombin substrate that is cleaved at physiologically relevant rates and affinity. The kinetics of thrombin cleavage of pure TR78 were monitored by HPLC analysis of base-quenched reaction products taken at various time points. Under conditions of dilute thrombin (100 pM), two HPLC peaks appeared and were confirmed by N-terminal sequence analysis and mass spectrometry to be TR62 (residues 42−103) and TR16 (residues 26−41) formed by the expected cleavage between $R_{41}-S_{42}$. Cleavage at R41 was linear for at least 30 min, and k_{cat} and K_M were determined to be 120 ± 7 s^{-1} and 16 ± 3 μM, respectively (Table 2). The catalytic efficiency, k_{cat}/K_M (= 7.5×10^6 M^{-1} s^{-1}), is within a factor of 2 compared to k_{cat}/K_M obtained for in vitro fibrinogen cleavage by thrombin (Table 2) and is 3-fold higher than a value (k_{cat}/K_M ~2.2×10^6 M^{-1} s^{-1}) obtained previously (*17*) for a shorter PAR1 exodomain (residues $A_{26}-Q_{81}$). Thus TR78 is recognized and cleaved by thrombin with a specificity constant that falls within biologically valid values. By using a ^{14}C-serotonin release assay, we also tested whether the soluble receptor exodomains could activate intact thrombin receptors on platelet membranes. The concentration of TR62 needed to activate platelets (EC_{50} ~40 μM) is comparable to that of SFLLR (EC_{50} ~50 μM)[2]. Not surprisingly, the full-length TR78 is unable to elicit a response even at concentrations as high as 75 μM. These results suggest that soluble TR78 and TR62 fragments are functional analogues of the resting and activated states, respectively, of the intact receptor extracellular domain.

[2] Unpublished experiments, S. K. Seeley, J. Baleja, and A. Kuliopulos.

Table 2: Kinetics of Thrombin and Plasmin Cleavage of the Soluble PAR1 Exodomain[a]

substrate	protease	cleavage sites	k_{cat} (s^{-1})	K_M (μM)	k_{cat}/K_M (M^{-1} s^{-1})	relative k_{cat}/K_M
TR78	thrombin	R41	120 ± 7	16 ± 3	7.5×10^6	1.0
TR62[b]	thrombin	R46, K76	$3.3 \times 10^{-3} \pm 0.4 \times 10^{-3}$	12 ± 4	2.8×10^2	$10^{-4.4}$
fibrinogen[c]	thrombin	AαR16	77 ± 2	5.7 ± 0.5	13.5×10^6	1.8
fibrinogen[d]	thrombin	AαR16	17.5×10^6	2.3		
TR78[e]	plasmin	K32, R41, R70, K76, K82	30 ± 3	18 ± 5	1.7×10^6	0.23
TR78[e]	plasmin	R70, K76, K82	16 ± 3	17 ± 11	9.4×10^5	0.13
TR78	plasmin	R41	13 ± 3	19 ± 6	6.8×10^5	0.09
TR62[e]	plasmin	R70, K76, K82	11 ± 3	20 ± 10	5.5×10^5	0.07
fibrinogen[f]	plasmin	αK206[g], βR42	0.48	0.42	1.1×10^6	0.15

[a] Cleavage reactions were performed in 20 mM KPO_4, pH 7.5, 150 mM NaCl, at 37 °C. The time courses of substrate cleavage at indicated sites were determined by HPLC analysis of NaOH-quenched aliquots as in Figure 1A. [b] Kinetic parameters, k_{cat} ($= k_2 + k_4$) and K_M ($\sim(K_1 + K_3)/2$), of combined secondary thrombin cleavages at R46 and K76, were determined by kinetic simulation of TR62 disappearance using the KINSIM numerical integration program according to the 2-site kinetic model of eq 1. Thrombin concentration varied from 1 to 5 μM, and TR62 concentration varied from 20 to 100 μM in seven separate experiments. Kinetic constants used for the best fit of eq 1 were $K_1 = 14$ μM, $k_2 = 0.002$ s^{-1}, $K_3 = 10$ μM, $k_4 = 0.0017$ s^{-1}, $K_5 = 20$ μM, and $K_6 = 10$ μM. The error is ±20% for each constant. [c] Kinetics of release of fibrinopeptide A from fibrinogen $(A\alpha B\beta\gamma)_2$ by HPLC assay in 5 mM Tris, 200 mM NaCl, 0.1% PEG, pH 8.0, 25 °C, with 0.2−10 nM thrombin (fast form) (E. Di Cera[3]). [d] Kinetics of release of fibrinopeptide A from fibrinogen $(A\alpha B\beta\gamma)_2$ by HPLC assay in 5 mM Tris, 200 mM NaCl, 0.1% PEG, pH 8.0, 37 °C, with 0.2−10 nM thrombin (fast form) (E. Di Cera[3]). [e] Kinetic parameters, apparent k_{cat} and apparent K_M, of combined plasmin cleavages at the P1−P3 (R70 + K76 + K82), and P1−P5 (K32 + R41 + R70 + K76 + K82) sites were directly determined under initial velocity conditions by the method of initial rates (*8*). Combined plasmin cleavage at P1−P3 was followed by integration of a single HPLC peak containing all three C-terminal fragments, TR33 + TR27 + TR21, resulting from cleavage at R70, K76, and K82, respectively (see Figure 1). Combined plasmin cleavage at P1−P5 was monitored by the disappearance of the TR78 starting material. Human plasmin concentration was 10 nM, and soluble PAR1 exodomain substrate concentration was varied from 14 to 100 μM. The initial velocities obtained at reaction times of ≤5 min were plotted as a function of exodomain concentration by double-reciprocal plots. [f] Generation of fragment X from 1 to 20 nM fibrinogen by 1 nM plasmin in the presence of 0.1 or 0.3 M NaCl, 50 mM Tris-HCl, pH 7.4, and 5 mM $CaCl_2$ (*50*). [g] Fragment X can also be produced by plasmin cleavage at sites located to the N-terminal side of K206.

Cleavage of Soluble PAR1 Exodomains by Anticoagulant Serum Proteases. The major anticoagulant serum proteases are (1) thrombin in complex with thrombomodulin, (2) activated protein-C, (3) tissue plasminogen activator (and urokinase plasminogen activator), and (4) plasmin. These tightly regulated serum proteases were assessed for their ability to truncate soluble PAR1 exodomains. In preliminary studies (*25*) we showed that micromolar thrombin cleaved TR62 at two specific secondary cleavage sites (R46 and K76) distal to the ligand. We have extended these studies and have now determined the kinetics of thrombin secondary cleavage. The catalytic efficiency of thrombin cleavage at these sites is 25000-fold slower than cleavage at the primary R41 site (Table 2). We then tested if thrombomodulin could enhance the ability of thrombin to cleave the soluble exodomain at the secondary cleavage sites since thrombomodulin is known to increase thrombin cleavage of protein-C by 20000-fold (*6*). Instead, the addition of 1.2 equiv of thrombomodulin has a 25% inhibitory effect on the thrombin secondary cleavage rates (data not shown). Due to the extremely slow rates of secondary thrombin cleavage in the presence or absence of thrombomodulin, it is unlikely that thrombin shuts off PAR1 by exodomain truncation.

Activated protein-C (APC) was also evaluated for its ability to cleave TR78 and TR62. There is no detectable cleavage of TR62 by 200 nM APC. However, APC is able to cleave TR78 at R41 (Table 1) at rates of approximately 1.3 min^{-1} which is 5000-fold slower than thrombin cleavage at the same site. There is no detectable (<1.9 h^{-1}) cleavage of TR78 by 2 μM tissue plasminogen activator. The final anticoagulant protease candidate to be tested was plasmin. As shown in Figures 1A and 2A, 10 nM plasmin is able to efficiently cleave TR62. The three cleavage peptide HPLC peaks were shown by MALDI-TOF mass spectrometry to contain 6 peptides resulting from cleavage at 3 clustered basic amino acids, residues R70, K76, and K82 (Table 1, Figure 1B). Plasmin cleavage at these sites was specific since there is no observed cleavage (<1%) at three other potential Arg- and Lys-cleavage sites after 4 h of incubation with plasmin. Notably, there is no observed cleavage at the secondary thrombin-cleavage site at R46, indicating different site preferences between thrombin and plasmin. Under initial velocity conditions, the apparent K_M and k_{cat} values based on the disappearance of TR62 are 20 μM and 11 s^{-1}, respectively (Table 2).

To rule out that our observed cleavages were due to a contaminating protease, we used the serpin, α_2-antiplasmin, to inhibit the cleavage reactions. When present in huge excess, α_2-antiplasmin can react with and form stable inactive complexes with other serum proteases including kallikrein, factor X_a, thrombin, urokinase, and t-PA. However, only plasmin is fully inactivated within 1 min incubation periods by nanomolar inhibitor (*7*, *48*). The addition of 1.8 equiv (18 nM) of human α_2-antiplasmin completely inhibited plasmin cleavage of TR62 within 1 min, and <0.2% cleavage was observed over 60 min incubation periods (data not shown). Contamination of the plasmin sample with thrombin was ruled out by chromogenic assays[4] using the thrombin specific substrate Spectrozyme TH (≤0.1% hydrolysis by plasmin) ±hirudin. Therefore, it is unlikely that a contaminating serum protease could be responsible for these cleavages.

We also wanted to test the hypothesis that plasmin could potentially desensitize unactivated receptors using the soluble TR78 fragment as a model for the resting state of the receptor exodomain. Plasmin cleaved the full-length TR78 exodomain more efficiently than TR62 as assessed by direct measurements of the initial rates of appearance of cleavage peptides

[3] Personal communication, E. Di Cera.

[4] Unpublished data, R. Jenny.

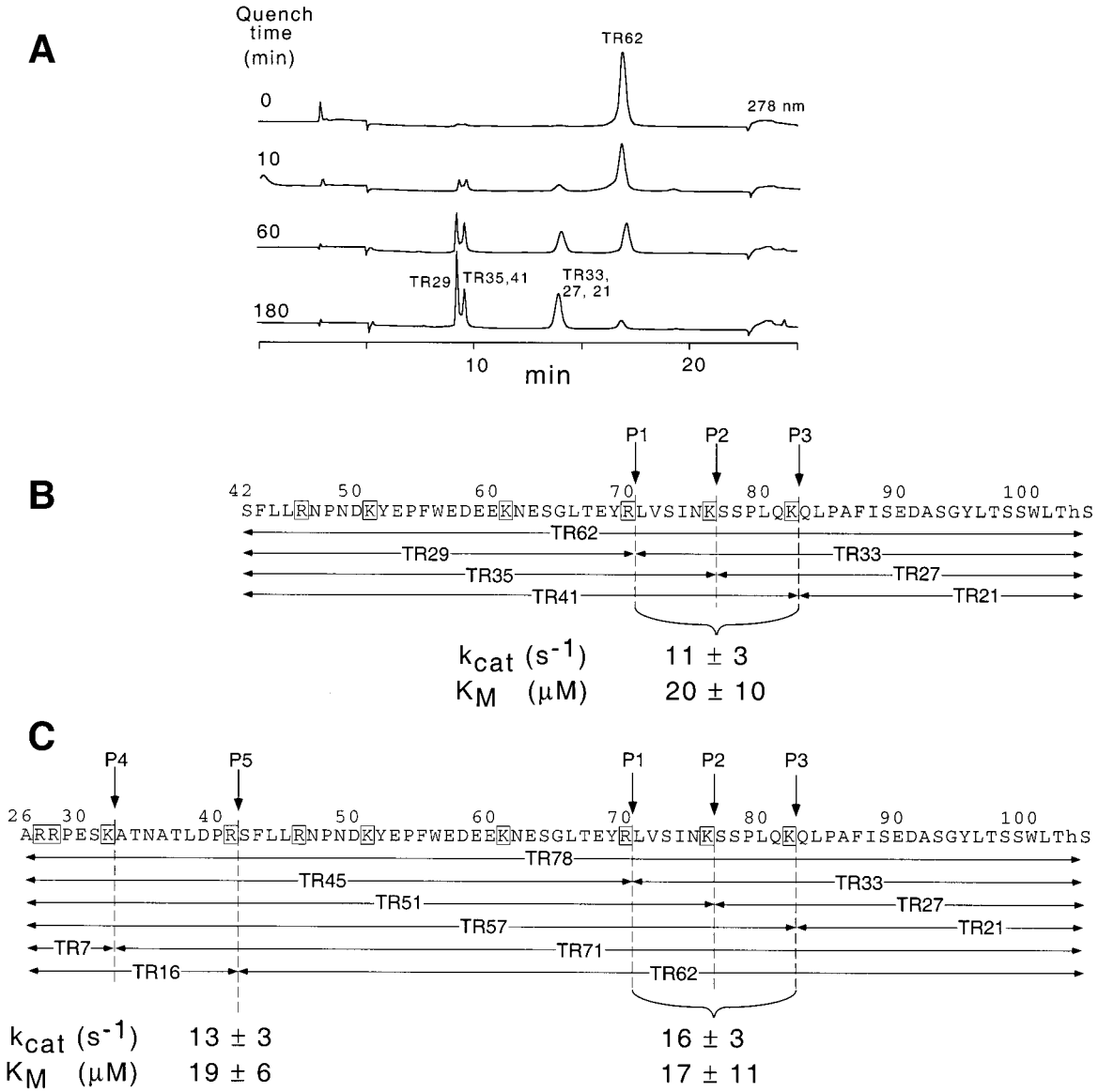

FIGURE 1: Plasmin cleavage of the PAR1 exodomain in resting and activated states. Cleavage reaction mixtures contained 10 nM human Lys-plasmin, 50 μM TR62 or TR78, in PBS, pH 7.5, 37 °C. The kinetics of plasmin cleavage of the resting form of the exodomain, TR78, and the activated form, TR62, were followed by HPLC analysis of base-quenched aliquots removed at various time points from cleavage reactions. TR62 and TR78 plasmin-cleavage sites and cleavage peptides were determined by MALDI mass spectrometry as listed in Table 1. The P1−P5 sites indicate plasmin-susceptible bonds. The C-terminal 'hS' residue designates the homoserine group generated by CNBr cleavage from the parent fusion construct. (A) Sequential HPLC chromatograms of TR62 cleavage by plasmin. (B) Location and kinetic parameters of plasmin cleavage at sites P1−P3 of TR62. (C) Location and kinetic parameters of plasmin cleavage at sites P1−P5 of TR78. For simplification, not all peptide fragments that were detected (Table 1) are shown.

resulting from combined cleavage at the P1−P5 sites (Figures 1C, 2B). The apparent K_M was unchanged (18 ± 5 μM) relative to that found for TR62, but the apparent k_{cat} was 3-fold faster at 30 ± 3 s^{-1} (Table 2). The relative k_{cat}/K_M of plasmin cleavage at the P1−P3 truncation sites was 2-fold faster for TR78 than for TR62. In addition to the same P1−P3-cleavage sites found earlier for TR62, other products were formed by cleavage of TR78 at K32 and R41 (Figure 1C, Table 2). The specificity of plasmin remained high with no observable cleavage (<1%) at R27, R28, R46, K51, or K61 during 4 h incubation periods. Cleavage at K32 is quite minor and contributes to only 1/500 of the overall initial rate of TR78 cleavage. Interestingly, plasmin cleavage at the R41 primary thrombin-cleavage site (P5) is comparable in both rate (13 s^{-1}) and affinity (19 μM) to the combined cleavage at the P1−P3 sites (Table 2). Cleavage at R41 resulted in a measurable but transient appearance of TR62 due to rapid C-terminal cleavage at the P1−P3 sites (Figure 2B). At the $t_{1/2}$ point of 16 min for TR78 cleavage, the TR62 species accounts for about 5% of the cleaved exodomain peptide products under our conditions.

Activation and Inhibition of Platelet Aggregation by Plasmin. As a first test of the validity of the relative plasmin and thrombin-cleavage rates determined using soluble exodomain, we compared the ratio of thrombin activation versus plasmin inhibition of platelets co-incubated with both proteases. Incubation of platelets with varying concentrations of plasmin confirmed that plasmin inhibits thrombin-induced platelet aggregation (Table 3). As predicted by the in vitro data, at very high concentrations, plasmin concomitantly induces direct aggregation of the platelets, consistent with cleavage of PAR1 at R41. At equimolar (10 nM) plasmin

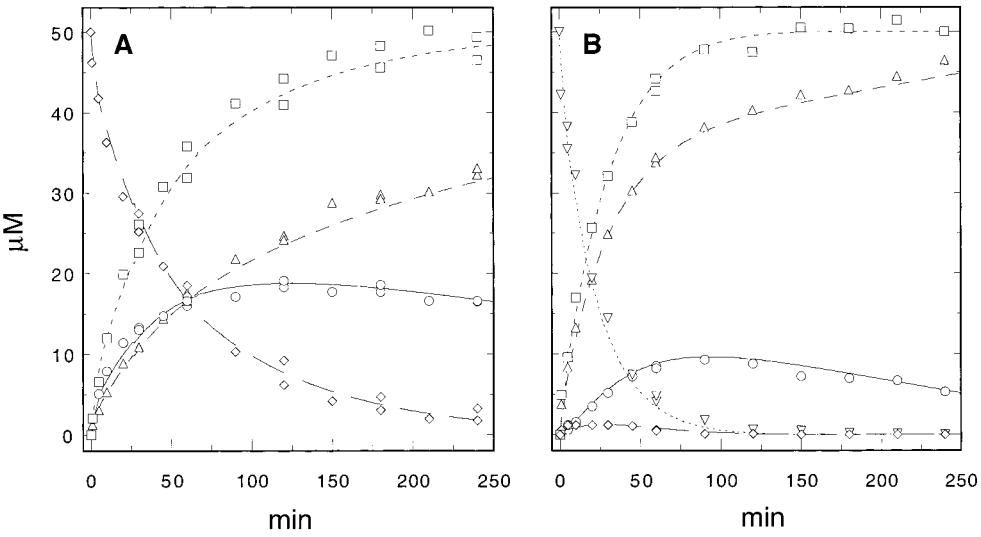

FIGURE 2: Time courses of plasmin cleavage of TR62 and TR78. Cleavage conditions were identical to those described in Figure 1. (A) Plasmin cleavage of 50 μM TR62 by 10 nM plasmin. These data are representative of 11 separate experiments: TR62 (◇); TR33 + TR27 + TR21 (□); TR29 (△); TR35 + TR41 (○). (B) Plasmin cleavage of 50 μM TR78 by 10 nM plasmin. These data are representative of 4 separate experiments: TR78 (▽); TR62 (◇); TR33 + TR27 +TR21 (□); TR29 + TR45 + TR38 + TR51 (△); TR35 + TR44 (○).

Table 3: Plasmin Both Inhibits Thrombin-Induced Platelet Aggregation and Directly Causes Platelet Aggregation[a]

	% platelet aggregation		% thrombin activation[b]
	no thrombin added	+ 10 nM thrombin	% plasmin inactivation
0 nM plasmin	0	88	–
10 nM plasmin	2	83	16
100 nM plasmin	3	74	5.1
300 nM plasmin	36	65	1.3

[a] Platelet-rich plasma was prepared from normal human donors and purified by gel filtration. The purified platelets were separated into 500 μL aliquots and recalcified by the addition of 2 mM $CaCl_2$. Platelet-poor plasma was prepared by centrifugation of the purified platelets at 14000*g* for 5 min and served as the blank. Stirred platelets were preincubated with varying concentrations of plasmin or water for 5 min at 37 °C before the addition of 10 nM human α-thrombin. The percent platelet aggregation was determined by the percent of light transmittance in a Bio/Data PAP-4 aggregometer (Horsham, PA) while continuously stirring at 900 rpm at 37 °C. The data were calibrated against the platelet-poor plasma blank and reported as the percent platelet activation reached at 5 min after the addition of thrombin (or water); 100% platelet aggregation was attained at about 10 min with 10 nM thrombin + 0 nM plasmin. Each data point was the mean of 3 samples run simultaneously. The error (2 standard errors) was ±5% of the mean. [b] The contribution of plasmin-induced platelet aggregation was subtracted from the thrombin-induced aggregation in the numerator.

and thrombin the ratio of thrombin activation of the platelets to plasmin inactivation of the platelets is 16. When 30-fold excess of plasmin relative to thrombin is used, the ratio decreases to 1.3. The level of direct plasmin activation of platelets varies from 2% to 36% as plasmin concentration increases from 10 to 300 nM.

Plasmin/t-PA Desensitization of the Ca^{2+} Response of Platelet Thrombin Receptors. Next, we more fully examined the effects of plasmin and t-PA/plasminogen on Ca^{2+} signaling in platelets. Gel-purified platelets were challenged with physiologically relevant (3 nM) thrombin concentrations at which the platelets become approximately 50% aggregated. Intracellular calcium levels were monitored by fura-2 fluorescence and are reported as the ratio of fluorescence intensity I340/380 (bound/free) (*13*). Platelets challenged sequentially with 3 nM thrombin (T) and 30 μM SFLLRN undergo immediate (<1 s) and very rapid increases in intracellular Ca^{2+} with initial velocities of calcium influx of 30−40 nM/s (Figure 3A). Pretreatment of the platelets with plasmin (P) inhibited the Ca^{2+} response to thrombin (Figure 3A). The inhibition was dependent on plasmin concentration with a IC_{50} of 50 ± 15 nM (Figure 3B). At this IC_{50} concentration of 50 nM, plasmin activates 10% of the platelet Ca^{2+} response. Extremely high plasmin concentrations (600 nM) result in up to 60% activation of platelets relative to thrombin, consistent with plasmin cleavage at the R41 site on PAR1. Plasmin activation (EC_{50} ~480 nM) of the platelet Ca^{2+} response is 75-fold less efficient than thrombin.

Remarkably, plasmin does not attenuate the response to SFLLRN. This would rule out classical homologous desensitization (i.e., receptor phosphorylation) of the platelet PAR1 by plasmin acting as a weak agonist (Figure 3B). By contrast, 3 nM thrombin desensitizes 75% of the SFLLRN response, and higher amounts of thrombin (>10 nM) desensitize up to 95% of the SFLLRN response by homologous desensitization. Since plasmin completely desensitizes the thrombin response and not the SFLLRN peptide response, this agrees with the in vitro data that the sites of plasmin cleavage are C-terminal to the tethered ligand but N-terminal to ligand-binding sites in PAR1 (Figure 7). In addition to lowering the peak intracellular Ca^{2+}, plasmin also inhibits the initial velocity of the Ca^{2+} flux in response to thrombin without inhibiting the initial velocity of the SFLLRN Ca^{2+} response (Figure 3A). This is consistent with competition of plasmin for thrombin recognition/cleavage sites without interfering with intermolecular liganding to SFLLRN.

To test the possibility that plasmin effects can also be induced by t-PA, we preincubated platelets with varying amounts of t-PA in the presence of physiological plasminogen (Plg) concentrations (1.2 μM). A range of t-PA concentrations were chosen that span those achieved during thrombolytic therapy. Similar to plasmin, the t-PA/Plg system efficiently attenuates the thrombin response. As shown in Figure 3C, t-PA causes a concentration-dependent inhibition

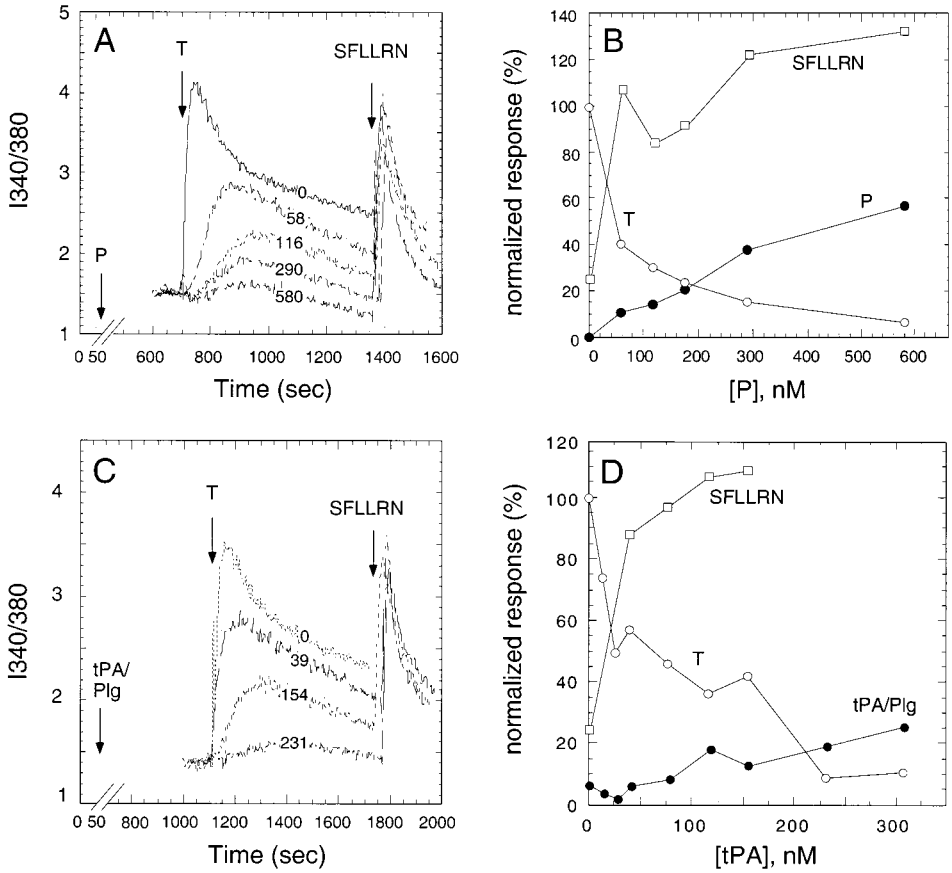

FIGURE 3: Plasmin/t-PA desensitization of the thrombin-induced Ca^{2+} response of platelets. Gel-filtered platelets were loaded with fura-2/AM and pretreated with the indicated nanomolar plasmin concentrations (A) or with tissue plasminogen activator (t-PA) in the presence of 1.2 μM plasminogen (C), and then challenged with 3 nM thrombin, followed by 30 μM SFLLRN. Intracellular Ca^{2+} was monitored as the ratio of fluorescence excitation intensity at 340/380 nm. The normalized responses to thrombin (T), SFLLRN, plasmin (P), or t-PA + 1.2 μM plasminogen (Plg) of the ΔI $340/380_{max}$ from the data of A and C are plotted as a function of plasmin (B) or t-PA (D), respectively. For purposes of clarity, the portions of the Ca^{2+} traces that show direct activation of platelets by plasmin have been omitted from A and C. The data shown are from several experiments using platelets from different volunteers.

of the Ca^{2+} response to thrombin with half-maximal inhibition at 44 ± 27 nM t-PA. This IC_{50} concentration is well below levels that are achieved in patients undergoing thrombolytic therapy with 50 mg bolus doses of t-PA whose initial t-PA plasma concentrations are 144 ± 53 nM t-PA (*44*). Likewise, a newer slower clearing form of t-PA, TNK-tPA, which is administered as a single 50 mg bolus injection, gives peak plasma levels of 160 nM (*28*). The clinical data indicate that, at early times during t-PA administration, the patient's platelets are exposed to sufficient quantities of t-PA that could induce plasmin truncation of platelet thrombin receptors. As is observed for plasmin alone, there is no effect on the SFLLRN response with t-PA pretreatment (Figure 3D). In the absence of plasminogen, t-PA had no effect on the thrombin or SFLLRN responses of platelets as predicted by the lack of cleavage of the soluble exodomain by t-PA.

Plasmin and Thrombin Cleavage of Full-Length PAR1 Expressed in Yeast. Having shown that plasmin can cleave the soluble PAR1 exodomain at the R70/K76/K82 sites and can inhibit platelet thrombin responses, we wanted to directly determine whether plasmin cleaves these same sites in full-length, membrane-embedded receptor. Since mammalian cell-expressed PAR1 is heavily glycosylated and migrates as several species on SDS−PAGE (see below), we initially tested nonglycosylated receptor in yeast (*42*) in order to simplify the interpretation of the cleavage data which has been difficult to interpret in previous proteolytic studies (*46*). Moreover, unlike platelets or mammalian cells maintained in cell culture, yeast has no prior contact with serum proteases or protease inhibitors, nor does yeast have endogenous protease receptors such as PAR1−4. To monitor cleavage at the R41 site of full-length receptor, a T7 epitope tag replaced PAR1 residues $A_{26}-N_{35}$ at the receptor N-terminus. As mentioned above, similar replacements had no effect on thrombin cleavage or receptor activation on PAR1 expressed in RAT1 or COS7 cells (*17*). Cleavage at the R70/K76/K82 sites was monitored by the loss of the $S_{42}-F_{55}$ epitope which is recognized by the SFLLR-Ab (*42*).

Wild-type (WT) receptor was expressed in yeast and membrane proteins purified as described (*42*). As predicted, treatment of the WT receptor with 5 nM thrombin results in ≥95% loss of the T7 epitope; however the SFLLR epitope is retained, indicating that thrombin cleaves solely at R41 (Figure 4A). Due to the removal of the 26 N-terminal amino acids, cleavage at the R41 site by thrombin (or plasmin) results in a slight downward shift from 33.8 kDa to 31.6 kDa in relative molecular mass as detected by the SFLLR-Ab. This polyclonal antibody stains the R41-cleaved receptor approximately 25% more intensely than the uncleaved receptor (Figure 4), consistent with increased accessibility to the authentic $S_{42}-F_{55}$ epitope.

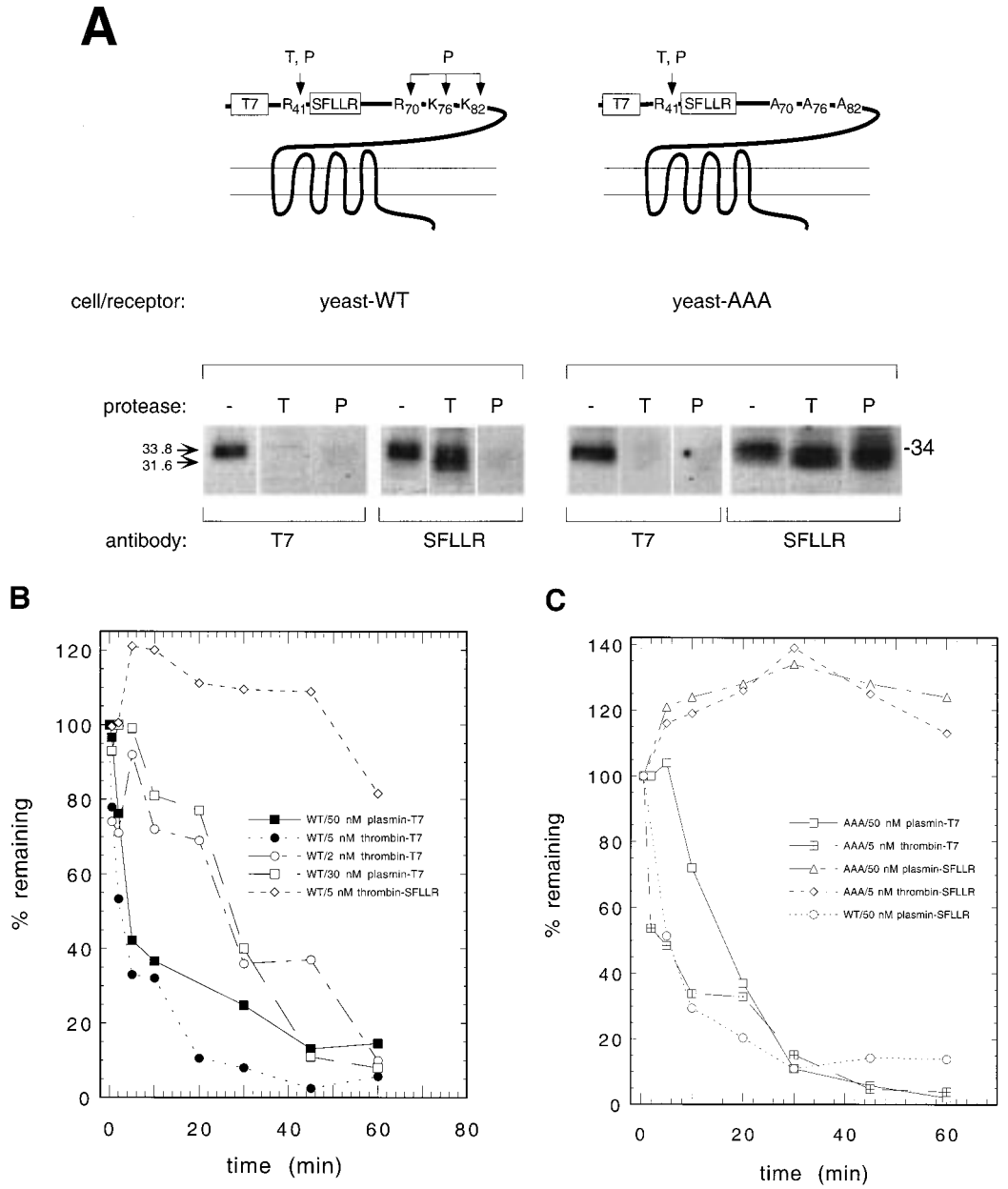

FIGURE 4: Plasmin and thrombin cleavage of PAR1 expressed in yeast membranes. (A, top) Schematic of the wild-type (WT) and triple-alanine (R70K76K82 → A70A76A82) mutant (AAA) PAR1 expressed in yeast. For monitoring cleavage by thrombin (T) and plasmin (P), the cleavage site at R41 is flanked by a T7 epitope (T7) and a $S_{42}-F_{55}$ epitope that includes the receptor ligand region (SFLLR). (A, bottom) Yeast membranes containing WT or AAA receptors were prepared and incubated with either 5 nM thrombin, 50 nM plasmin, or buffer for 1 h at 37 °C in 20 mM KPO_4, pH 7.5, 100 mM NaCl. Cleavage reactions (40 μg of total protein) were quenched with 4 M urea/SDS sample buffer and separated by 10% SDS−PAGE. Proteins were electroblotted onto PVDF membranes and probed with anti-T7 or anti-SFLLR antibodies. Kinetics of thrombin and plasmin cleavage of WT (B) and AAA (C) PAR1 in yeast membranes. Aliquots from cleavage reaction mixtures were removed at various times, quenched by 2-fold dilution into 8 M urea/SDS sample buffer, and analyzed by anti-T7 and anti-SFLLR westerns as above. Band intensity was quantitated by densitometry of autoradiographs and is normalized to 100% at $t = 0$ min.

Treatment of the WT receptor with plasmin results in about 90% loss of both T7 and SFLLR epitopes, in agreement with cleavage occurring at the R41 and R70/K76/K82 sites. Mutation of these potential plasmin-cleavage sites to A70/A76/A82 (AAA mutant) allowed us to distinguish between cleavage at the R41 site versus the R70/K76/K82 sites. Membrane fractions containing the AAA mutant receptor were produced and treated with either thrombin or plasmin. As shown in Figure 4A, thrombin and plasmin removed the T7 epitope; however, neither protease cleaved to the C-terminal side of the SFLLR epitope in the AAA mutant. From these data, we can conclude that plasmin can cut only at R41 in the AAA mutant. Therefore, the R70/K76/K82 sites are the only sites of plasmin truncation in full-length, yeast-produced receptor.

It was also convenient to use the yeast-expressed receptors to measure relative rates of plasmin and thrombin cleavage at the R41 and R70/K76/K82 sites in the context of the nonglycosylated full-length receptor. Thrombin cleavage of the WT receptor at the R41 site is approximately 10−15-fold faster than cleavage by plasmin at all four combined sites (Figure 4B, Table 4). As expected, thrombin cleaves the AAA mutant at the R41 site at essentially the same rate as in WT (Table 4). By comparing the rates of T7 and

Table 4: Kinetics of Thrombin and Plasmin Cleavage of PAR1 Expressed in Various Cells

receptor	cell	protease	epitope monitored	$t_{1/2}$ (min)
WT	yeast	5 nM thrombin	T7	2.5 ± 0.5
WT	yeast	50 nM plasmin	T7	4.3 ± 0.9
WT	yeast	2 nM thrombin	T7	26 ± 5
WT	yeast	30 nM plasmin	T7	27 ± 5
AAA	yeast	5 nM thrombin	T7	3.0 ± 0.6
AAA	yeast	50 nM plasmin	T7	16 ± 3
WT	yeast	50 nM plasmin	SFLLR	5.4 ± 1.1
WT	yeast	100 nM plasmin	SFLLR	4.0 ± 0.8
WT	COS7	100 nM plasmin	SFLLR	2.0 ± 0.4
WT	HEL	100 nM plasmin	SFLLR	0.9 ± 0.2

SFLLR epitope loss, respectively, we determined that the rate of plasmin cleavage of the AAA mutant receptor at R41 is 3-fold slower than combined cleavage at the R70/K76/K82 sites in WT (Figure 4C, Table 4). For comparison, the analogous relative cleavage (k_{cat}/K_M) ratio of the soluble TR78 exodomain by plasmin is 1.4-fold. Plasmin cleavage at R41 in the AAA mutant is approximately 50-fold slower than thrombin cleavage at R41.

Plasmin and Thrombin Cleavage of Glycosylated PAR1 Expressed in COS7 Fibroblasts. Essentially nothing is known of the function, if any, of glycosylation on PAR1 activation and regulation. Thrombin receptor glycosylation has been proposed to play an important role in proteolysis, protein folding and/or protein transport, and stability (*46*). We know that PAR1 is highly glycosylated as indicated by abnormal mobility of the platelet, HEL, and COS7-produced receptor under denaturing conditions (Figure 5). PAR1 has 5 potential N-linked glycosylation sites at residues 35, 62, 75, 250, and 259. None of these residues are conserved. The actual site(s) of linkage are not known; however, glycosidase studies of PAR1 indicate that there is at least one site of N-linked glycosidation (*46*). Treatment of PAR1 with N-glycosidase removed the vast majority of the glycosyl moieties, indicating that serine/threonine *O*-glycosyl linkages have a negligible contribution. Three of the potential N-linked sites (N35, N62, and N75) are located in the PAR1 N-terminal exodomain which might potentially affect plasmin cleavage—especially at K76 which is adjacent to N75 (Figure 7).

We tested whether plasmin could cleave at the R70/K76/K82 sites in fully glycosylated, mammalian cell-expressed receptor and compared the cleavage rates with those occurring in the nonglycosylated yeast-produced receptor. We have confirmed that plasmin cleaves the identical R70/K76/K82 sites in the fully glycosylated COS7-expressed receptor. As shown in Figure 5A,B, the transiently expressed PAR1 is heterogeneously glycosylated; however, a minor nonglycosylated component migrates at the relative molecular weight (34 kDa) identical to that which occurs in yeast. For comparison, the platelet-produced receptor migrates as a more homogeneous species at 75 kDa. Addition of 20 nM thrombin results in a shift in relative MW from 103 kDa to a series of bands ranging from 50 to 100 kDa. Since this shift in relative MW is much greater than the 2.2 kDa shift observed upon thrombin cleavage of the nonglycosylated receptor, it identifies N35 as one of the sites of N-linked glycosylation. Furthermore, we can also conclude that PAR1 has additional site(s) of N-linked glycosylation to the C-terminal side of R41 since the thrombin-cleaved PAR1 migrates as a much larger species than the nonglycosylated receptor. Incubation of the WT receptor with 300 nM plasmin results in >96% loss of the SFLLR epitope, indicating that glycosylation of the receptor does not adversely affect plasmin cleavage at the R70/K76/K82 sites. Mutation of the three plasmin-cleavage sites to A70/A76/A82 abrogates plasmin truncation of the receptor. As in the yeast-expressed receptor, plasmin can still cleave the COS7 cell-produced AAA mutant at the R41 thrombin-cleavage site (Figure 5A).

The kinetics of plasmin cleavage of the transiently expressed receptor were compared to cleavage of endogenous receptor expressed in human erythroblastic leukemia (HEL) cells. As shown in Figure 5B,C, 100 nM plasmin removes the SFLLR epitope from recombinant and endogenous receptor within 5 min time periods. Plasmin-catalyzed loss of the SFLLR ligand region is 2−4-fold faster than the rate of cleavage of the nonglycosylated receptor under the same conditions (Table 4). These data demonstrate that the extensive glycosylation of the mammalian cell-produced receptor does not protect against plasmin cleavage at the P1−P3 sites located within the exodomain linker region.

Plasmin Truncates and Desensitizes Wild-Type PAR1 and Activates a Triple Alanine Mutant (R70K76K82 → A70A76-A82) Receptor Expressed on Intact Cells. We tested whether plasmin cleaves PAR1 at the P1−P3 and R41 (P5) sites on the receptor expressed on intact mammalian cells. The plasmin-cleavage sites, R70/K76/K82, were mutated to alanine (AAA-PAR1), and plasmin desensitization of the Ca^{2+} response was compared with that of wild-type PAR1 in transiently transfected COS7 fibroblasts. The fraction of cells expressing PAR1 receptor on the plasma membrane (22%) was identical for WT and AAA-PAR1 as determined by flow cytometry using antibodies raised against the SFLLRN ligand region (Figure 6A). Plasmin cleavage of WT-PAR1 and AAA-PAR1 receptors on the surface of intact cells was quantified using flow cytometry. Transfected cells were incubated with either 100 nM plasmin, 300 nM plasmin, or 20 nM thrombin. As shown in Figure 6B, plasmin removes up to 55% the tethered ligand region from WT-PAR1, whereas the AAA-PAR1 is completely resistant to plasmin truncation. As monitored by the loss of a N-terminal T7-epitope tag, thrombin cleavage of AAA-PAR1 is not impaired by the triple-alanine mutation and the extent of cleavage is equivalent to the maximal loss seen with plasmin cleavage at the R70/K76/K82 sites. The remaining ~40% of the T7 and SFLLR epitopes are resistant to cleavage by very high concentrations of plasmin or thrombin, suggesting that a subset of the PAR1 exodomains may be in a protected environment as previously seen in platelets (*29*) and endothelial cells (*32*). These results, for the first time, directly show that plasmin cleaves the PAR1 receptor at the R70/K76/K82 sites on intact mammalian cells.

We then correlated the removal of the SFLLRN preligand region by plasmin with attenuation of the Ca^{2+} response. Plasmin-pretreated fibroblasts were challenged with thrombin or the SFLLRN peptide. Pretreatment with 116 nM plasmin for 2 min cause a 36% attenuation of the thrombin Ca^{2+} response in WT-PAR1/COS7 cells, but had no effect on AAA-PAR1/COS7 cells (Figure 6C). As before in the platelet experiments, pretreatment of WT-PAR1 or AAA-PAR1 transfected cells with 116 nM plasmin had little effect on the SFLLRN Ca^{2+} response, indicating that the removal of

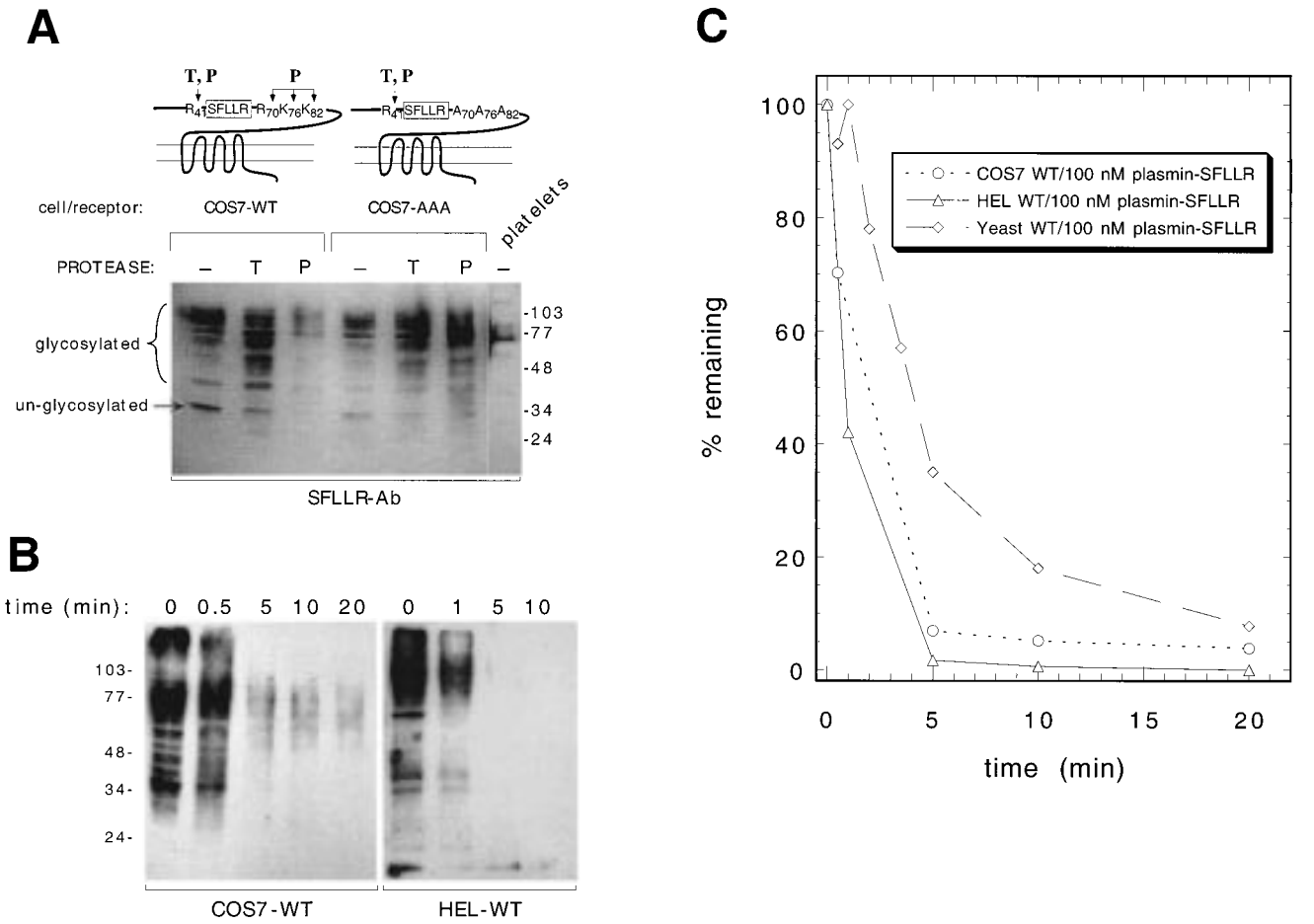

FIGURE 5: Plasmin and thrombin cleavage of PAR1 expressed in COS7 fibroblasts and HEL cells. Protease treatments were carried out on crude membranes prepared from HEL cells or COS7 cells transfected with the human WT or AAA PAR1. (A) Transiently transfected cells were treated for 15 min with 20 nM thrombin (T) or 300 nM plasmin (P) or buffer (−) for 1 h at 37 °C in 20 mM KPO_4, pH 7.5, 100 mM NaCl at 37 °C. The right lane contains crude membranes from human platelets. Cleavage reactions (40 μg of total protein) were quenched with 4 M urea/SDS sample buffer and separated by 10% SDS−PAGE. Proteins were electroblotted onto PVDF membranes and probed with anti-SFLLR antibodies as in Figure 4. (B) Kinetics of 100 nM plasmin cleavage of WT PAR1 expressed on COS7 and HEL cells. Aliquots from cleavage reaction mixtures were removed at various times, quenched by 2-fold dilution into 8 M urea/SDS sample buffer, and analyzed by anti-SFLLR westerns as in Figure 4. (C) Time course of the disappearance of the SFLLR epitope following 100 nM plasmin treatment of PAR1 on yeast, HEL, and COS fibroblasts cell membranes.

residues N-terminal to Q83 does not affect activation by the intermolecular ligand.

Mutation of the R70/K76/K82 sites might also be expected to increase the ability of plasmin to act as an agonist by cleavage at the R41 site and thereby convert PAR1 to a "plasmin receptor". Indeed, treatment of the AAA-PAR1/COS7 cells with plasmin elicits 90−120% of the corresponding Ca^{2+} response to thrombin (Figure 6D). WT-PAR1/COS7 cells are only 50−60% activated by plasmin relative to the Ca^{2+} response to 10 nM thrombin. Together, these results validate that the mechanism of plasmin attenuation of the PAR1 thrombin response on intact cells is due to cleavage at the R70/K76/K82 sites and that plasmin can also activate the thrombin receptor by cleavage at R41.

DISCUSSION

The present work has established that plasmin desensitizes PAR1 by cleavage at three clustered arginine and lysine residues located to the C-terminal side of the tethered ligand region and N-terminal to ligand-binding sites. Mutation of these three residues to alanine abolishes plasmin truncation and desensitization of thrombin-dependent Ca^{2+} signaling. Ex vivo Ca^{2+} studies of human platelets confirmed that plasmin completely desensitizes all platelet thrombin responses without affecting intermolecular liganding of PAR1. Plasmin, generated by subtherapeutic levels of t-PA, is equally effective in desensitizing all platelet thrombin responses. Higher concentrations of plasmin activate platelets consistent with cleavage at the R41 site of PAR1. This would explain the seemingly contradictory behavior of t-PA/plasmin on platelets, namely, that low concentrations of t-PA/plasmin inhibits platelet function, whereas high concentration of t-PA/plasmin activates platelets.

Using the soluble receptor exodomain as a model for proteolytic activation/deactivation of the full-length receptor has allowed us to rapidly screen various proteases for their ability to truncate PAR1. This approach allowed us to unambiguously determine cleavage sites, rates, and relative specificities among these proteases. The data presented here demonstrate that, of the anticoagulant proteases, only plasmin can efficiently truncate the soluble PAR1 exodomain both in resting and in activated states. We confirmed that plasmin can cleave at the R70/K76/K82 truncation sites in full-length membrane-embedded receptor regardless of the state of glycosylation.

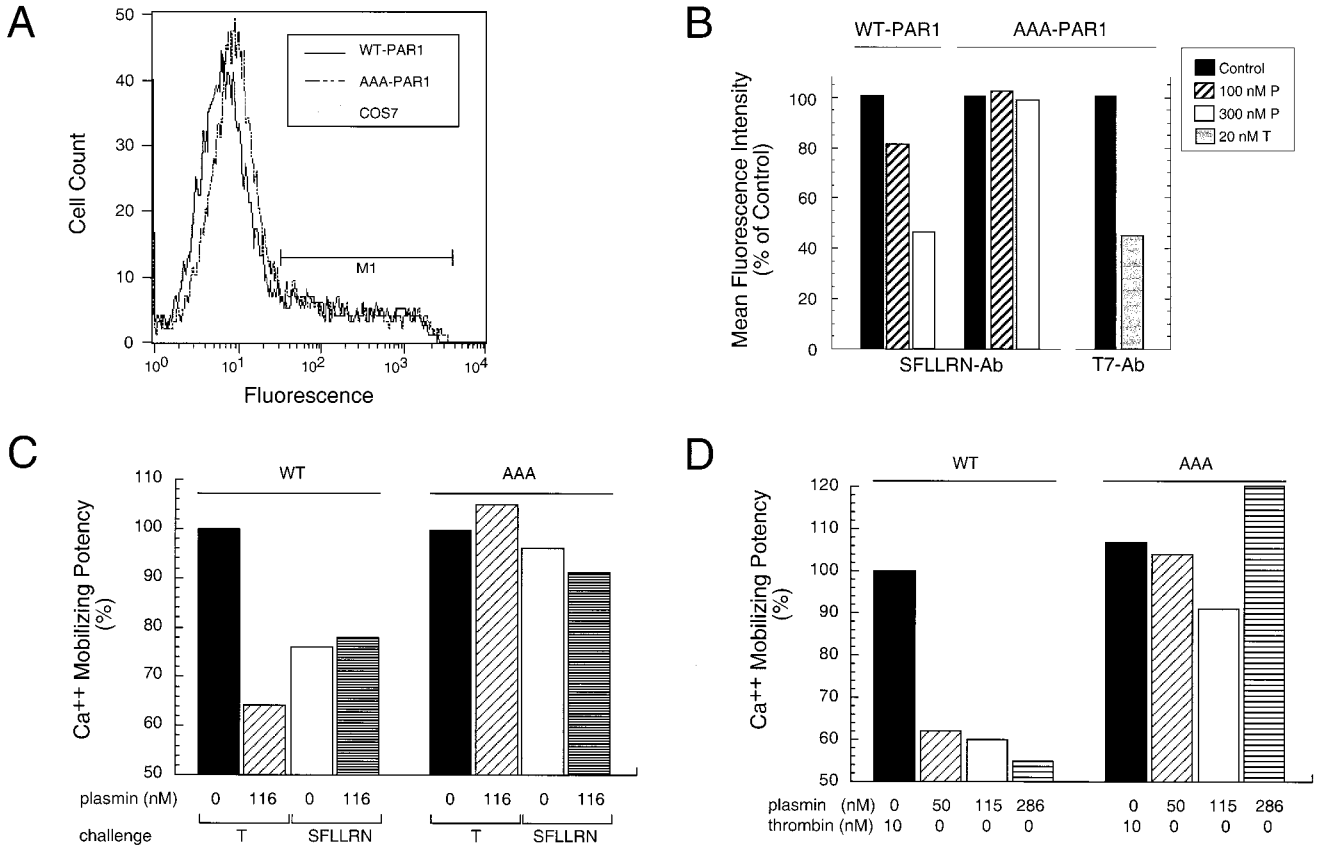

FIGURE 6: Mutation of the R70/K76/K82 sites abrogates plasmin truncation and desensitization of PAR1 expressed on the surface of intact cells. COS7 cells were transfected with the pcDEF3 vector expressing wild-type human PAR1 (WT-PAR1) or the triple alanine mutant receptor (AAA-PAR1). The next day, cells were replated at a density of 1×10^6 cells/10 cm plate. After 24 h, cells were incubated with either 100 nM plasmin (P), 300 nM P, 20 nM thrombin (T), or PBS buffer (control) for 15 min at 37 °C, 5% CO_2. Retention of the SFLLRN ligand region or of a N-terminal T7 epitope tag was monitored by flow cytometry with anti-SFLLRN polyclonal antibodies or with a monoclonal anti-T7 antibody, respectively. (A) Transiently transfected COS7 WT-PAR1 cells, AAA-PAR1 cells, or nontransfected COS7 cells were incubated with SFLLRN-Ab, washed twice, and then incubated with goat antirabbit IgG-FITC and analyzed by flow cytometry. (B) The mean fluorescence intensities of the gated cells marked as M1 using the SFLLRN-Ab (A) or the T7-Ab (data not shown). Data are expressed as relative shifts in mean fluorescence intensity compared with the corresponding values from protease-untreated control cells. (C) Plasmin desensitization of the thrombin response of intact COS7 cells expressing PAR1 was monitored by the integrated Ca^{2+} signal (Ca^{2+} Mobilizing Potency-CMP). Upon recovering from transfection (after 3 days), Ca^{2+} fluorescence measurements were conducted as described in the Methods Section. Cells were pretreated with 0 or 116 nM plasmin for 2 min and challenged with 10 nM thrombin or 30 μM SFLLRN. (D) Plasmin activation of the Ca^{2+} response of the AAA-PAR1 or WT-PAR1 expressed in COS7 fibroblasts. Cells were treated with the indicated concentrations of plasmin or thrombin; 100% of the integrated Ca^{2+} response (CMP) is defined as the CMP of cells challenged with 10 nM thrombin.

How do the kinetics of plasmin truncation of the soluble PAR1 exodomain compare with plasmin cleavage of the soluble form of fibrin, namely, fibrinogen? Although there is scarce kinetic data available for plasmin cleavage of fibrinogen, a recent study determined the rate constants, k_{cat} and K_D, of fragment X formation to be 0.48 s^{-1} and 0.42 μM, respectively (*50*). The second-order rate constant, k_{cat}/K_D is calculated to be 1.1×10^6 M^{-1} s^{-1}. For comparison, the k_{cat}/K_M of plasmin truncation of TR62 and TR78 is 0.6−0.94×10^6 M^{-1} s^{-1} (Table 2). Therefore, the rates of plasmin P1−P3 cleavage of the soluble PAR1 exodomains are nearly identical to that of an authentic plasmin substrate, fibrinogen. Moreover, it is important to note that plasmin ($K_M = 20$ μM) has essentially the same affinity as thrombin ($K_M = 16$ μM) for the soluble PAR1 exodomain. Therefore, one would predict that plasmin would truncate the thrombin-cleaved receptor exodomain about 14-fold slower (k_{cat}/K_M of 120 s^{-1}/16 μM versus 11 s^{-1}/20 μM) than thrombin activation of full-length membrane-embedded exodomain given saturating amounts of competing proteases. The overall catalytic efficiency, k_{cat}/K_M, of plasmin P1−P3 cleavage of TR78 is 2-fold higher than plasmin cleavage of TR62 and only 8-fold lower than cleavage of TR78 by thrombin. Therefore, under conditions of near-equimolar thrombin and plasmin, cleavage by plasmin may become kinetically and physiologically significant. Our platelet aggregation studies provide the initial evidence that these relative cleavage rates may be valid in vivo since competing thrombin and plasmin give activation/deactivation ratios varying from 1.3 to 16 depending on relative molarity (Table 3). In the ex vivo experiments described in Figure 3, pretreatment of platelets with plasmin gave an IC_{50} value of 50 nM for the desensitization of the thrombin Ca^{2+} response. The corresponding EC_{50} for thrombin was 6.5 nM in untreated platelets. This would give a thrombin EC_{50}/plasmin IC_{50} ratio of 8 which is in perfect agreement with the predicted ratio based on relative cleavage rates of the soluble exodomain.

Two previous studies detected plasmin cleavage at the R41 site of shorter synthetic peptides containing residues FP_{40}−F_{55} (*20*) and L_{38}−E_{60} (*37*) of PAR1. In the first study by Kimura and colleagues (*20*), plasmin was used to generate active peptide ligand (S_{42}−F_{55}) in situ from the FP_{40}−F_{55}

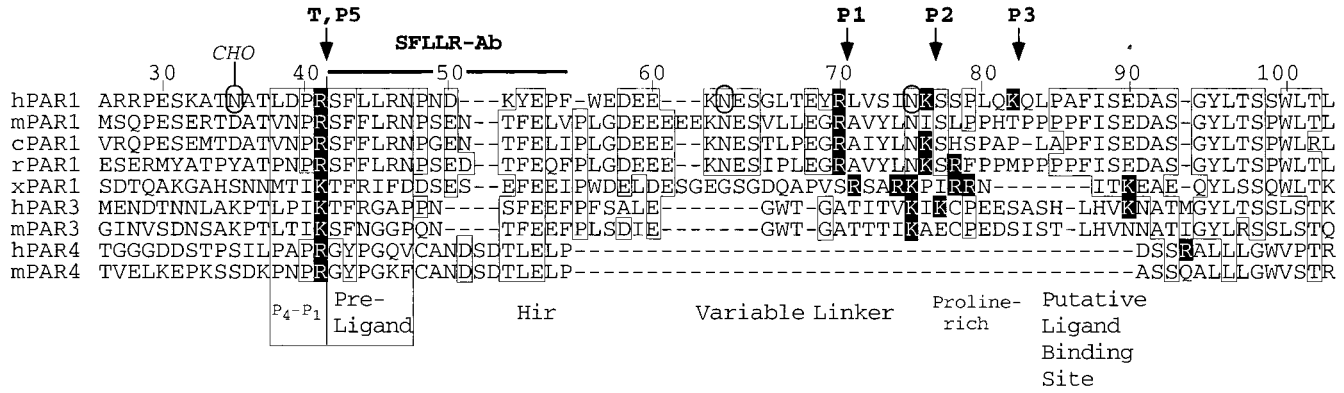

FIGURE 7: Alignment of thrombin receptor exodomains. T is the primary thrombin-cleavage site, and P1, P2, P3, and P5 are the major plasmin-cleavage sites of the human PAR1 N-terminal exodomain. The thrombin receptor exodomain sequences are human (h), mouse (m), rat (r), hamster (c), and frog (x). Thrombin interacts with these exodomains at two sites: (1) the active site at XX(P/I)(R/K)(S/T/G) and (2) the fibrinogen recognition site at the hirudin-like (Hir) region, X(Y/F/L)EX(F/I/V/P). Cleavage at the T/P5-cleavage site exposes the (S/T/G)(F/Y)XXXX N-terminal ligand that is postulated to activate the receptor by either direct or indirect interaction with ligand-binding sites, one of which comprises residues 85−89 in hPAR1. The blackened basic amino acids indicate previously identified or potential protease-susceptible cleavage sites located adjacent to a proline-rich "linker" region that separates the putative ligand-binding site from the N-terminus of the exodomain. "CHO" indicates an identified site of N-linked glycosylation, and the ellipsoids indicate potential sites of N-linked glycosylation.

inactive precursor as assessed by Ca^{2+} responses of platelets. They did not provide kinetic data for the assessment of the efficiency of plasmin cleavage at R41. In the second study by Parry et al. (*37*), the authors obtained a k_{cat}/K_M value for plasmin cleavage of a 23-mer peptide that was 1700-fold lower relative to thrombin cleavage at R41. In our kinetic studies, which employ the entire exodomain of PAR1, plasmin cleaves at the R41 site only 10-fold less efficiently than thrombin. To explain this 170-fold discrepancy in plasmin cleavage at R41, we suggest that plasmin recognizes binding determinants located to the N-terminal side of L38, or that the TR78 exodomain provides structural determinants[2] lacking in the synthetic 23-mer peptide used by Parry et al. Our work would thereby provide a reasonable explanation for the enigma that plasmin can both deactivate and weakly activate platelets and endothelial cells in vivo (*3*, *33*).

Kimura and colleagues (*20*) also provided circumstantial evidence that plasmin can remove or alter the PAR1 $K_{34}-R_{46}$ preligand epitope from the platelet surface. Treatment of the platelets with 134 nM plasmin for 15 min resulted in 40% loss of the $K_{34}-R_{46}$ epitope as determined by flow cytometry. The anti-$K_{34}-R_{46}$ antibody could not distinguish between complete loss of this region by C-terminal cleavage, insertion of the epitope into a protected pocket, and cleavage simply at R41; however, the time course of the plasmin-induced loss of the preligand epitope correlated well with the attenuation of the subsequent thrombin response. Strictly speaking, these kinds of antibody studies cannot be interpreted solely in terms of PAR1 cleavage since receptor activation by thrombin results in a conformation change that can bury ligand epitopes without much effect at other extracellular epitopes (*35*). Moreover, there is at least one other protease-susceptible thrombin receptor (i.e., PAR3, PAR4) that could have cross-reactivity with ligand-specific antibodies (*15*, *40*). Given the complexity of the protease responses of these cells, it will be essential to establish the cleavage kinetics of each protease receptor in isolation in order to fully understand how the cellular arm of the hemostatic system is controlled.

Last, our finding that plasmin cleavage occurs at three clustered basic residues, R70, K76, and K82, suggests that the PAR1 extracellular domain contains a protease-susceptible linker. This region coincides with a proline-rich sequence and is located just N-terminal to the putative ligand-binding site located in the C-terminal portion of the exodomain (*1*, *9*, *34*). A homology alignment of the human PAR1 extracellular domain with all known thrombin receptors with the exception of PAR4 indicates that R70 and/or K76 are conserved in an otherwise poorly homologous region (Figure 7). This provides suggestive evidence that these potential serum protease-cleavage sites have been preserved for purposes of rapid receptor desensitization.

ACKNOWLEDGMENT

We thank Margaret Jacobs for peptide synthesis and sequencing and Steffen Helmling for help in the construction of the PAR1 exodomain fusion proteins.

REFERENCES

1. Bahou, W. F., Kutok, J. L., Wong, A., Potter, C. L., and Coller, B. S. (1994) *Blood 84*, 4195−4202.
2. Barshop, B. A., Wrenn, R. F., and Frieden, C. (1983) *Anal. Biochem. 130*, 134−145.
3. Chang, W.-C., Shi, G.-Y., Chou, Y.-H., Chang, L.-C., Hou, J.-S., Lin, M. T., Jen, C. J., Wing, L.-Y. C., and Wu, H.-L. (1993) *Am. J. Physiol. 264*, C271−C281.
4. Collen, D. (1997) *Thromb. Haemostasis 78*, 742−746.
5. Coller, B. S., Ward, P., Ceruso, M., Scudder, L. E., Springer, K., Kutok, J., and Prestwich, G. D. (1992) *Biochemistry 31*, 11713−11720.
6. Dahlback, B., and Stenflo, J. (1994) in *The Protein C Anticoagulant System* (Stamatoyannopoulos, G., Nienhuis, A. W., Majerus, P. W., and Varmus, J., Eds.) pp 599−627, W. B. Saunders, Philadelphia, PA.
7. Edy, J., and Collen, D. (1977) *Biochem. Biophys. Acta 484*, 423−432.
8. Fersht, A. (1985) in *Enzyme Structure and Mechanism*, pp 121−154, W. H. Freeman and Company, New York.
9. Gerszten, R. E., Chen, J., Ishii, M., Ishii, K., Wang, L., Nanevicz, T., Turck, C. W., Vu, T.-K. H., and Coughlin, S. T. (1994) *Nature 368*, 648−651.
10. Gimple, L. W., Gold, H. K., Leinbach, R. C., Coller, B. S., Werner, W., Yasuda, T., Johns, J. A., Ziskind, A. A., Finkelstein, D., and Collen, D. (1989) *Circulation 80*, 582−588.

11. Goldman, L. A., Cutrone, E. C., Kotenko, S. V., Krause, C. D., and Langer, J. A. (1996) *BioTechniques 21*, 1013−1015.
12. Greco, N. J., Jones, G. D., Tandon, N. N., Kornhauser, R., Jackson, B., and Jamieson, G. A. (1996) *Biochemistry 35*, 915−921.
13. Grynkiewicz, G., Poenie, M., and Tsien, R. Y. (1985) *J. Biol. Chem. 260*, 3440−3450.
14. Ishihara, H., Connolly, A. J., Zeng, D., Kahn, M. L., Zheng, Y. W., Timmons, C., Tram, T., and Coughlin, S. R. (1997) *Nature 386*, 502−506.
15. Ishihara, H., Zeng, D., Connolly, A. J., Tam, C., and Coughlin, S. R. (1998) *Blood 91*, 4152−4157.
16. Ishii, K., Chen, J., Ishii, M., Koch, W. J., Freedman, N. J., Lefkowitz, R. J., and Coughlin, S. R. (1994) *J. Biol. Chem. 269*, 1125−1130.
17. Ishii, K., Gerszten, R., Zheng, Y. W., Welsh, J. B., Turck, C. W., and Coughlin, S. R. (1995) *J. Biol. Chem. 270*, 16435−16440.
18. Ishii, K., Hein, L., Kobilka, B., and Coughlin, S. R. (1993) *J. Biol. Chem. 268*, 9780−9786.
19. Kahn, M. L., Zheng, Y.-W., Huang, W., Bigornia, V., Zheng, D., Moff, S., Farese, R. V., Tam, C., and Coughlin, S. R. (1998) *Nature 394*, 690−694.
20. Kimura, M., Andersen, T. T., Fenton, J. W., Bahou, W. F., and Aviv, A. (1996) *A. J. Physiol. 271*, C45−C60.
21. Kinlough-Rathbone, R. L., Perry, D. W., Rand, M. L., and Packham, M. A. (1997) *Thromb. Haemostasis 77*, 741−747.
22. Kozak, M. (1990) *Proc. Natl. Acad. Sci. U.S.A. 87*, 8301−8305.
23. Kuliopulos, A., Mildvan, A. S., Shortle, D., and Talalay, P. (1989) *Biochemistry 28*, 149−159.
24. Kuliopulos, A., Nelson, N. P., Yamada, M., Walsh, C. T., Furie, B., Furie, B. C., and Roth, D. A. (1994) *J. Biol. Chem. 269*, 21364−21370.
25. Kuliopulos, A., and Sheridan, P. J. (1995) *Blood 86*, 448a.
26. Kuliopulos, A., and Walsh, C. T. (1994) *J. Am. Chem. Soc. 116*, 4599−4607.
27. Liu, L., Freedman, J., Hornstein, A., Dewar, L., Blajchman, M. A., and Ofosu, F. A. (1996) *Br. J. Haemostasis 92*, 458−465.
28. Modi, N. B., Eppler, S., Breed, J., Cannon, C. P., Braunwald, E., and Love, T. W. (1998) *Thromb. Haemostasis 79*, 134−139.
29. Molino, M., Bainton, D. F., Hoxie, J. A., Coughlin, S. R., and Brass, L. F. (1997) *J. Biol. Chem. 272*, 6011−6017.
30. Molino, M., Barnathan, E. S., Numerof, R., Clark, J., Dreyer, M., Cumash, A., Hoxie, J. A., Schechter, M., Woolkalis, M., and Brass, L. F. (1997) *J. Biol. Chem. 272*, 4043−4049.
31. Molino, M., Blanchard, N., Belmonte, E., Tarver, A. P., Abrams, C., Hoxie, J. A., Cerletti, C., and Brass, L. F. (1995) *J. Biol. Chem. 270*, 11168−11175.
32. Molino, M., Woolkalis, M. J., Reavey-Cantwell, J., Pratico, D., Andrade-Gordon, P., Barnathan, E. S., and Brass, L. F. (1997) *J. Biol. Chem. 272*, 11133−11141.
33. Nakamura, K., Kimura, M., Fenton, J. W., Andersen, T. T., and Aviv, A. (1995) *Am. J. Physiol. 267*, 958−967.
34. Nanevicz, T., Ishii, M., Wang, L., Chen, M., Chen, J., Turck, C. W., Cohen, F. E., and Coughlin, S. R. (1995) *J. Biol. Chem. 270*, 21619−21625.
35. Norton, K. J., Scarborough, R. M., Kutok, J. L., Escobedo, M.-A., Nannizzi, L., and Coller, B. S. (1993) *Blood 82*, 2125−2136.
36. Nystedt, S., Emilsson, K., Wahlestedt, C., and Sundelin, J. (1994) *Proc. Natl. Acad. Sci. U.S.A. 91*, 9208−9212.
37. Parry, M. A. A., Myles, T., Tschopp, J., and Stone, S. R. (1996) *Biochem. J. 320*, 335−341.
38. Schafer, A. I., and Adelman, B. (1985) *J. Clin. Invest. 75*, 456−461.
39. Schafer, A. I., Rodriguez, R., Loscalzo, J., and Gimbrone, M. A. (1989) *Blood 74*, 1015−1020.
40. Schmidt, V. A., Nierman, W. C., Maglott, D. R., Cupit, L. D., Moskowitz, K. A., Wainer, J. A., and Bahou, W. F. (1998) *J. Biol. Chem. 273*, 15061−15068.
41. Serebruany, V. L., Gurbel, P. A., Shustov, A. R., Dalesandro, M. R., Gumbs, C. I., Grabletz, L. B., Bahr, R. D., Ohman, E. M., and Topel, E. J. (1998) *Stroke 29*, 235−238.
42. Sheridan, P. J., Swift, S., Covic, L., Seeley, S. K., and Kuliopulos, A. (1998) (submitted for publication).
43. Suidan, H. S., Bouvier, J., Schaerer, E., Stone, S. R., Monard, D., and Tschopp, J. (1994) *Proc. Natl. Acad. Sci. U.S.A. 91*, 8112−8116.
44. Tebbe, U., Tanswell, P., Seifried, E., Feuerer, W., Scholz, K.-H., and Herrmann, K. S. (1989) *Am. J. Cardiol. 64*, 448−453.
45. Turner, J. S., Redpath, G. T., Humphries, J. E., Gonias, S. L., and Vandenberg, S. R. (1994) *Biochem. J. 297*, 175−179.
46. Vouret-Craviari, V., Grall, D., Chambard, J.-C., Rasmussen, U. B., Pouyssegur, J., and Obberghen-Schilling, E. V. (1995) *J. Biol. Chem. 270*, 8367−8372.
47. Vu, T.-K. H., Hung, D. T., Wheaton, V. I., and Coughlin, S. R. (1991) *Cell 64*, 1057−1068.
48. Wiman, B. (1981) *Methods Enzymol. 80*, 395−408.
49. Woolkalis, M. J., Jr., T. M. D., Blanchard, N., Hoxie, J. A., and Brass, L. F. (1995) *J. Biol. Chem. 270*, 9868−9875.
50. Wu, J.-H., and Diamond, S. L. (1995) *Anal. Biochem. 224*, 83−91.
51. Xu, W.-F., Andersen, H., Whitmore, T. E., Presnell, S. R., Yee, D. P., Ching, A., Gilbert, T., Davie, E. W., and Foster, D. C. (1998) *Proc. Natl. Acad. Sci. U.S.A. 95*, 6642−6646.

BI9824792